# Journal Pre-proof

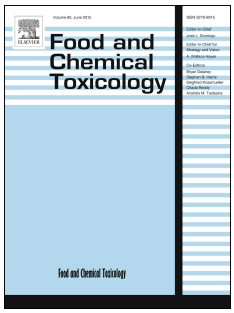


Impaired ferritinophagy flux induced by high fat diet mediates hepatic insulin resistance via endoplasmic reticulum stress

Chunjie Jiang, Shanshan Zhang, Dan Li, Li Chen, Ying Zhao, Guibin Mei, Jingjing Liu, Yuhan Tang, Chao Gao, Ping Yao

PII: S0278-6915(20)30217-9

DOI: https://doi.org/10.1016/j.fct.2020.111329

Reference: FCT 111329

To appear in: *Food and Chemical Toxicology*

Received Date: 12 February 2020

Revised Date: 5 April 2020

Accepted Date: 6 April 2020

Please cite this article as: Jiang, C., Zhang, S., Li, D., Chen, L., Zhao, Y., Mei, G., Liu, J., Tang, Y., Gao, C., Yao, P., Impaired ferritinophagy flux induced by high fat diet mediates hepatic insulin resistance via endoplasmic reticulum stress, *Food and Chemical Toxicology* (2020), doi: https://doi.org/10.1016/j.fct.2020.111329.

**Chunjie Jiang:** Writing - Original Draft, Methodology, Formal analysis, Investigation

**Shanshan Zhang:** Methodology, Formal analysis, Investigation

**Dan Li:** Methodology, Investigation

**Li Chen:** Methodology, Investigation

**Ying Zhao:** Methodology, Investigation

**Guibin Mei:** Methodology, Investigation

**Jingjing Liu:** Methodology

**Yuhan Tang:** Writing - Review & Editing

**Chao Gao:** Conceptualization, Resources, Writing - Review & Editing, Project administration, Funding acquisition

**Ping Yao:** Conceptualization, Resources, Writing - Review & Editing, Supervision, Project administration, Funding acquisition

# Impaired ferritinophagy flux induced by high fat diet mediates hepatic insulin resistance via endoplasmic reticulum stress

Chunjie Jiang[a], Shanshan Zhang[c], Dan Li[a], Li Chen[a], Ying Zhao[a], Guibin Mei[a], Jingjing Liu[a], Yuhan Tang[a], Chao Gao[b]*, Ping Yao[a]*

[a] Department of Nutrition and Food Hygiene, School of Public Health, Tongji Medical College, Huazhong University of Science and Technology, Wuhan, China

[b] National Institute for Nutrition and Health, Chinese Center for Disease Control and Prevention, Beijing, China

[c] Laboratory Animal Platform of Academy of Medical Sciences, Zhengzhou University, Zhengzhou, China

*Corresponding author:

Prof. P. Yao E-mail addresses: yaoping@mails.tjmu.edu.cn

Ministry of Education Key Laboratory of Environment School of Public Health

Tongji Medical College, Huazhong University of Science and Technology Wuhan, China

Dr. C. Gao E-mail addresses: gaochao20090901@163.com

National Institute for Nutrition and Health, Chinese Center for Disease Control and Prevention, Beijing, China



DFO deferoxamine
ERS Endoplasmic reticulum stress
FAC Ferric ammonium citrate
HFD high-fat diet
IR Insulin resistance
LIP Labile iron pool

## Abstract

Although iron disequilibrium has been observed frequently in high-fat diet (HFD) related insulin resistance (IR) the exact mechanism still obscure. Herein, we explore the potential mechanism, focusing on hepatic ferritinophagy flow. Male C57/6J mice were administered with HFD or low-fat diet (LFD) for 10 weeks, and HepG2 cells were treated with palmitate (PA, 200 mM) for 24 hours. HFD led to abnormal hepatic steatosis and decline p-AKT and p-GSK3β by 67.1% and 66.3%, respectively. Also, not only decreased iron level but increased endoplasmic reticulum stress (ERS) were observed in the liver of HFD mice and that both them impaired glucose uptake and reduced the expression of p-AKT. However, ferric ammonium citrate (FAC) supplementation improved hepatic IR, as well as ERS. What's more, HFD/PA depleted the labile iron pool (LIP), accumulated p62 and disturbed the expression of nuclear receptor coactivator 4 (NCOA4) and ferritin. While NCOA4 overexpression or rapamycin improved the ERS and impaired glucose uptake in PA incubated HepG2 cells, which was abolished by NCOA4 knockdown or bafilomycin A1. Taken together, these findings suggest that HFD could restrict ferritinophagy flux and interfere with iron metabolism, which resulting in hepatic IR via ERS.

**Keywords:** ferritinophagy flux; nuclear receptor coactivator 4; endoplasmic reticulum stress; hepatic insulin resistance; high-fat diet

## 1. Introduction

Insulin resistance (IR) is a common feature of metabolic disorders including obesity, nonalcoholic fatty liver disease (NAFLD) and diabetes, which contribute to the major public health issue in the world (Samuel & Shulman, 2016). The main target of IR includes skeletal muscle, white adipose tissue and liver, and in particular, the liver is crucially responsible for systemic glucose homeostasis by producing glucose during fasting and stores glucose (Petersen & Shulman, 2017). And the liver is the source of 70% of endogenous glucose during fasting (Magnusson, Rothman, Katz, Shulman, & Shulman, 1992). Thus, hepatic IR has been assumed as one of the main intervention targets for various chronic metabolic diseases.

Iron is an essential micro-element. On one hand, several studies found that excessive iron deposition may be one of the risk factors for insulin resistance and diabetes (Simcox & McClain, 2013; Zhou et al., 2019). On the other hand, the deficiency of iron could initiate a variety of metabolic changes on lipid and glucose metabolisms besides typical iron deficiency anemia (Kamei et al., 2010). Recently, iron dysregulation has been frequently observed during the progression and development of chronic metabolic diseases. Epidemiological investigations revealed that iron deficiency is common in obesity, which may be caused by increased hepcidin induced by chronic low-grade inflammation(Cheng, Bryant, Cook, O'Connor, Rooney, & Steinbeck, 2012; Manios et al., 2013). Emerging laboratory studies showed that iron was decreased as a consequence of chronic high-fat diet (HFD) regime or palmitate (PA) treatment (Jung et al., 2015; Sonnweber et al., 2012). Also, PA could

deplete intracellular labile iron pool (LIP) and that iron supplementation significantly protects cells from death(Jung et al., 2015).

Endoplasmic reticulum stress (ERS) has been well accepted as one of the central pathways to stimulate hepatic IR (O. K. Kim, Jun, & Lee, 2015; Lee, 2017). It was frequently reported that iron chelation induced apoptosis via the ERS pathway (J. L. Kim et al., 2016; Seo, Li, & Wessling-Resnick, 2013). In addition, our previous study revealed that ERS is involved in HFD induced hepatic steatosis and rescuing ERS improved hepatic IR (Yu et al., 2018; Zhu et al., 2018). We therefore suppose that iron deficiency induced by HFD may lead to hepatic IR via ERS. However, the exact mechanism of the iron disturbance in HFD induced hepatic IR is still unclear.

As a specific cargo receptor, nuclear receptor coactivator 4 (NCOA4) mediated ferritinophagy plays a critical role in intracellular and systemic iron homeostasis (Bellelli et al., 2016; Mancias, Wang, Gygi, Harper, & Kimmelman, 2014). Physiologically, iron is stored in ferritin when iron excess while during iron demand iron atoms could be released and that ferritin can store up to 4500 iron atoms(Arosio, Ingrassia, & Cavadini, 2009; Quiles Del Rey & Mancias, 2019). NCOA4 delivers ferritin to the lysosome and mediates the selective autophagic degradation of ferritin (Mancias et al., 2014). Besides, metabolically active forms of intracellular iron are components of a cytosolic labile iron pool (LIP), and iron released from degradation of ferritin induces an increase in cellular LIP (Konijn, Glickstein, Vaisman, Meyron-Holtz, Slotki, & Cabantchik, 1999). Our previous study showed that autophagy and mitophagy played an important role in HFD-induced hepatic steatosis

(Liu et al., 2018). However, it is not known whether ferritinophagy is involved in HFD induced hepatic IR. In the present study, we investigated the effect of iron dysregulation in HFD mice and PA incubated HepG2 cells on hepatic IR, focused on ferritinophagy regulation.

## 2. Materials and methods

### 2.1. Chemicals and reagents

Thapsigargin (TG), deferoxamine (DFO), ferric ammonium citrate (FAC) and NCOA4 antibodies were purchased from Sigma-Aldrich (USA). Dp44mT was purchased from Selleck chem (USA). Calcein-AM was obtained from Dojindo (Japan). Antibodies specific for GAPDH, p-AKT (Ser473), t-Akt, p-GSK3β, t-GSK3β, p-EIF2α, t-EIFα, p-IRE1α, t-IRE1α, XBP1 and p62 antibodies and horseradish peroxidase (HRP) secondary antibody were procured from Cell Signaling Technology (USA). Mouse antibodies specific for NCOA4, heavy-chain ferritin (HFT) and light-chain ferritin (LFT) were purchased from Abcam (USA). ATF6 and Grp78 antibodies were purchased from Santa Cruz Biotechnology Inc (USA). 2-NBDG was provided by Thermo Fisher (USA). Bafilomycin A1, Rapamycin, Wortmannin, 4-phenylbutyrate (4-PBA) and STF-083010 (STF) and MG-132 were purchased from MedChemExpress (USA). LysoTracker Red DND-99 (LTR), were purchased from Invitrogen. (USA)

### 2.2 Experimental Animal and Treatment

Five-week-old male C57BL/6J mice were purchased from Sino-British Siper/BK Lab Animal Ltd (Shanghai, China). All animals were treated following the

'Guiding Principles in the Care and Use of Animals' approved by Tongji Medical College Council on Animal Care Committee. The mice were housed with a 12 h light/dark cycle with free access to diets and water. The animals were randomly divided into two dietary groups (n = 10/group): (1) low-fat diet (LFD, 10% energy from fat); (2) HFD (60% of energy from fat). The low-fat diets (MD12031) and high-fat diets (MD12033) were purchased from the Medicience (Yangzhou, China). After 10 weeks, the liver tissues were collected. The diet composition as we previously described (Yu et al., 2018).

**2.3. Hematoxylin and eosin (H&E) staining**

H&E staining was performed as previously described (Zhu, Yao, Liu, Guo, Jiang, & Tang, 2020).

**2.4. Oral Glucose Tolerance Test (OGTT) and Insulin Tolerance Test (ITT)**

The OGTT and ITT were performed 1 week before mice sacrificed as previously described (Zhao et al., 2011). For OGTT, glucose 1.5 g/kg as a 50% w/v solution in water by oral administration. For ITT human insulin (0.75 IU/kg) was administrated by intraperitoneal injection. All the blood glucose level was measured from tail veins using Accu-Chek glucometer (Roche Diagnostics GmbH, Mannheim, Germany).

**2.5. Cell culture and treatment of palmitate**

HepG2 cells were maintained in DMEM with 10% fetal bovine serum (FBS), 1% v/v penicillin-streptomycin at 37°C and 5% CO2 atmosphere as previously described(Liu et al., 2018) HepG2 cells were cultured in 200μM PA or deferoxamine

(DFO, 50μM), ferric ammonium citrate (FAC, 10μM), 4-phenylbutyrate (4-PBA, 500μM), STF-083010 (STF, 100 μM), TG (1μM) MG132(10 μM), Bafilomycin A1 (Baf, 50 nM), Wortmannin (Wor, 200 μM ) and Rapamycin (Rapa, 100 nM) for 24h. And the cells were collected for bioassays.

For the preparation of PA: the palmitate (50 mM in 0.1 M NaOH) incubated at 70□ for 30 min complexed to fatty acid-free bovine serum albumin (BSA) (5.5 mM) at 37□ for 1h in a 2:3 volume ratio as previously described (Kwon, Lee, & Querfurth, 2014). The control BSA was prepared by mixing 1 mL of 0.1M NaOH and 1.5mL fatty acid-free BSA.

**2.6. Western Blot Analysis**

Liver tissues and HepG2 cells were homogenized and lysed in RIPA Lysis Buffer (1% Triton X-100, 1% deoxycholate, 0.1% SDS). The total protein extraction of the lysates was measured by BCA protein assay kit (Beyotime Biotechnology, China). Immunoblotting was performed as the manufacturer's guidelines (Bio-Rad, Hercules, CA). The membranes were blocked with a washing buffer (4 mM Tris–HCl, 30 Mm NaCl, 0.1% Tween-80, pH 7.6) containing 5% skimmed milk for 2h. And then each target band was incubated overnight at 4 °C with the specific antibody and 1h at room temperature with corresponding secondary antibody. The membranes were washed and detected subsequently with EGL plus kit in Western Blotting Detection System (Amersham Bioscience, Little Chalford, UK). Optical densities of the membranes were quantified by Image J software. The concentration of all the antibodies diluted according to the corresponding specifications.

**2.7. Total Hepatic Iron and Labile Iron Pool (LIP) Assay**

The total hepatic iron and LIP levels of the liver were determined according to our previous description(Tang et al., 2014). Iron sensitive fluorescent dye Calcein-AM

was used to determine the LIP level in HepG2 cells according to the previous description (Sturm, Goldenberg, & Scheiber-Mojdehkar, 2003).

**2.8. Glucose Uptake Assay**

After washing three times with PBS, the HepG2 cells were immediately incubated in KRBH buffer in the presence of 100 nM insulin before the addition of 2-NBDG (100 μ M) for 30 min at 37 °C as previously described (Q. Zhang et al., 2018). The images were obtained by an inverted fluorescence microscope (Olympus, Japan). And the software used to get images is MShot Image Analysis System.

**2.9. Immunofluorescence**

Liver tissues and HepG2 cells were processed as previously described (Liu et al., 2018). The primary antibodies used were Heavy chain-ferritin (1:200, Abcam), NCOA4 (1:200, Sigma-Aldrich) and LAMP2 (1:200, Santa Cruz) in 10% goat serum albumin at 4 °C overnight, followed by incubation with secondary antibodies for 2 h and DAPI (Beyotime) for 5min at room temperature. The secondary antibodies (1/800, Invitrogen) were as follows: Alexa fluro™ 647 goat anti-rat lgG, Alexa fluro™ 488 goat anti-rabbit IgG and Alexa fluor™ 555 goat anti-mouse IgG. The tissues were observed by a laser scanning confocal microscope (LSM 900 Carl Zeiss Inc., Germany) and the cells were photographed under an inverted fluorescent microscope (Olympus, Japan). And the software used to get images are ZEN 2012 and MShot Image Analysis System, respectively.

**2.10. Adenovirus-Mediated Overexpress of NCOA4 and siRNA-Mediated Knockdown of NCOA4 in HepG2 Cells**

NCOA4 Adenovirus (Ad-NCOA4, NM-005437.3) transfection: HepG2 cells were seeded onto 6-well plates, When HepG2 cells grown to 70%, the cells were transfected with Ad-NCOA4 or Ad-null (Vigene, Jinan, China) as previously described.

Human NCOA4 siRNA transfection: Once grown to 70% confluence in antibiotic□free medium, HepG2 cells were transfected with small interfering (si)-RNA against NCOA4 or scrambled siRNA using Lipofectamine® RNAiMAX (Invitrogen; USA) according to the manufacturer's protocol. And the si-h-NCOA4 purchased from RiboBio (Guangzhou, China; 5'- GCTCATGCTAGTTCAGCAA -3'). After 48h of transfection, the cells were treated with PA (200μM) with or without other intervention for 24 h. And the transfection efficiency was verified by western blot.

**2.11. Statistics**

The data are shown as the mean ± standard error (SEM). Data with two groups were compared using Student t test. Comparisons between multiple groups were assessed by One -way ANOVA with Bonferroni analysis. Statistical analysis was performed with prism 5.0. $P < 0.05$ was considered a statistically significant difference.

**3. Results**

**3.1 HFD induces Hepatic steatosis and insulin resistance in mice**

As shown in Fig.1A, mice fed with HFD showed a significantly higher body weight gain from the fifth week till the end of the experiment when compared with

LFD mice. ITT and OGT test (Fig. 1B and C) showed that HFD also decreased the Systematic insulin sensitivity. H&E staining (Fig. 1D) indicated that long term HFD leads to liver structural disorder and severe hepatic cell steatosis, which showed white vacuole-like changes. To further evaluate the underlying mechanism of glucose metabolism disorder, we measured the protein level of total and phosphorylated AKT and GSK3β in liver tissue. Interestingly, HFD declined p-AKT and p-GSK3β by 67.1% and 66.3%, respectively (Fig. 1E and F).

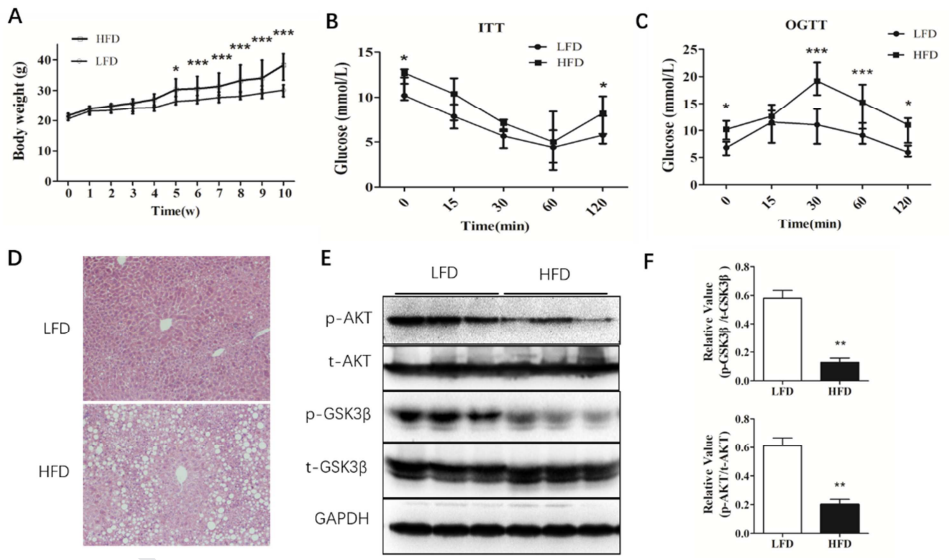


**Fig 1.** Hepatic insulin resistance in HFD mice. (A) Bodyweight of mice was measured weekly (n=10). (B, C) ITT and OGTT were tested during the ninth week (n = 6). Values were presented as means ± SEM. (D) hematoxylin-eosin staining of liver tissues. (E-F) The protein levels of p-AKT, t-AKT, p-GSK3β and t-GSK3β in the liver were determined by Western blot. Values were presented as means ± SEM. * $p < 0.05$; ** $p<0.01$; ***: $p<0.001$ versus the LFD group.

### 3.2 The effect of ERS and iron level on hepatic IR

To observe the effect of HFD on ERS, ERS-related proteins were evaluated by

western blot (Fig. 2A). As shown in Fig. 2B, HFD increased the expression of GRP78 by 38.9%. The expression of p-EIF2α slightly increased (Fig. 2E). However, HFD increased p-IRE1α, XBP-1 and ATF6α by 313%, 99.2% and 179.3 respectively (Fig. 2C, D and F). To verify the role of ERS induced by excessive lipid intake in hepatic IR in vitro, we evaluated the effect of 4-PBA, an inhibitor of ERS and STF, the IRE1α endonuclease inhibitor on p-AKT expression and glucose uptake level of HepG2 cells in the presence of PA. Both 4-PBA and STF improved p-AKT expression and glucose uptake levels in the presence of insulin. However, thapsigargin (TG), an inducer of ERS aggravated the impaired glucose uptake.

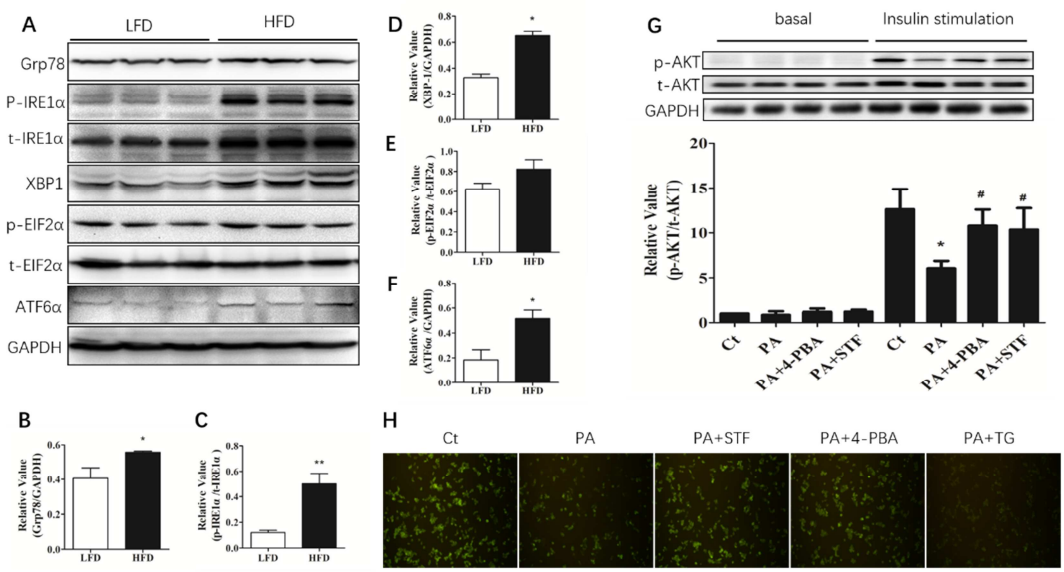


**Fig 2.** The effect of ERS on hepatic IR. (A-F) The protein levels of Grp78, p-IRE1α, XBP-1, p-EIF2α and ATF6α in mice were determined by Western blot. (G) p-AKT level in HepG2 cells. (H) The glucose uptake of HepG2 cells was tested in the presence of insulin. Values were presented as means ± SEM (n=3). * $p < 0.05$; ** $p<0.01$versus the LFD or Ct group. #: $p < 0.05$ versus the PA group.

To test the effect of HFD on the hepatic iron level, we measured the iron level

and found that HFD feeding decreased the total iron level and the protein of ferritin light-chain (L-Ferritin) to 75.2% and 34.2% respectively (Fig. 3A and B). In addition, we found that in HepG2 cells the LIP, a kind of freely exchangeable and available iron decreased in a PA dose-dependent manner (Fig. 3C). Moreover, iron supplementation with FAC reversed the expression of p-AKT and the glucose uptake in PA incubated HepG2 cells, and that deferoxamine (DFO), an iron chelator (Fig. 3D and E) further exacerbated the adverse effect.

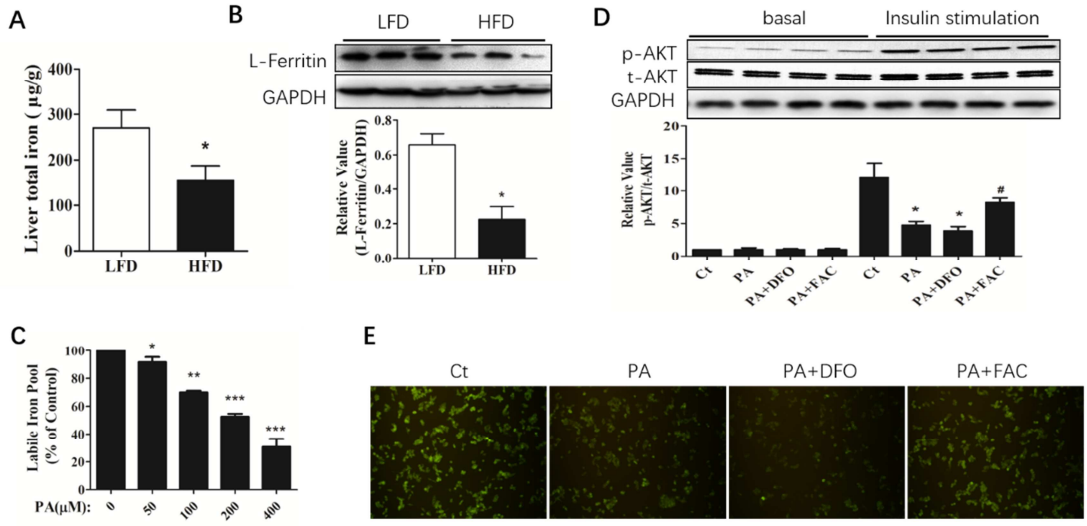


**Fig 3.** The effect of iron on hepatic IR. Liver total iron (A) were determined by flame atomic absorption spectrometry (n=8). (B) The protein level of the light chain of ferritin (L-Ferritin) (n=3). (C) LIP level in HepG2 cells was determined by fluorescent dye Calcein-AM. (D) p-AKT level of HepG2 cells. (E) The glucose uptake of HepG2 cells. The experiments were repeated 3 times. Values were presented as means ±SEM. *p < 0.05; ** p<0.01; ***: p<0.001 versus the LFD or Ct group. #: p < 0.05 versus the PA group.

### 3.3 Iron supplementation in PA incubated HepG2 cells improved ERS

We have observed that both decreased iron level and increased ERS could

induce hepatic IR *in vivo and in vitro*. To demonstrate the effect of iron level on ERS, we then evaluated the ERS level in HepG2 cells after treating with DFO or FAC in the presence of PA. As we showed in Fig.4A-C, PA treatment noticeably stimulated the p-IRE1α, p-EIF2α and XBP-1 but did not affect the expression of ATF6α (Fig. 4D). DFO incubation exacerbated the effect of PA while FAC reversed IRE1α phosphorylation and XBP-1 expression. Furthermore, FAC improved the impaired glucose uptake but showed no effect in the presence of TG. (Fig. 4F).

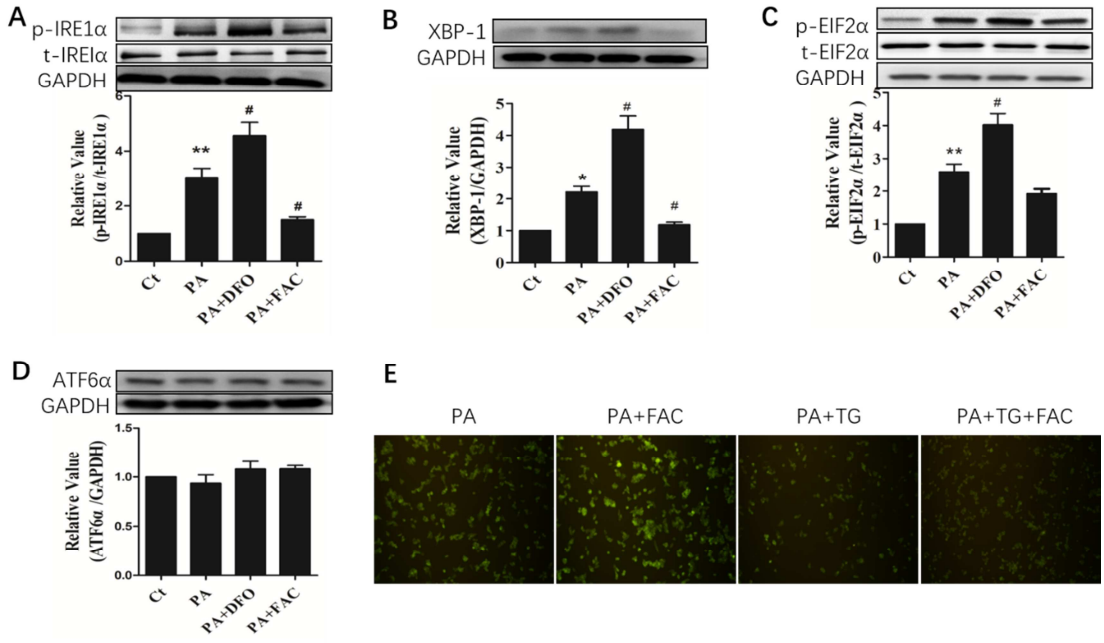


**Fig 4.** Iron supplementation in PA incubated HepG2 cells improved ERS. The protein levels of p-IRE1α, XBP-1, ATF6α and p-EIF2α (A, B, C, D) in HepG2 cells. (E) The glucose uptake of HepG2 cells was tested in the presence of insulin. The experiments were repeated 3 times. Values were presented as means ± SEM. * $p < 0.05$; ** $p<0.01$ versus the Ct group. #: $p < 0.05$ versus the PA group.

### 3.4 Ferritinophagy flux was suppressed *in vivo and vitro*.

Recent reports have demonstrated that NCOA4 is crucial for autophagic ferritin

degradation and that impaired NCOA4 function predisposes to iron recycling dysregulation(Bellelli et al., 2014). We therefore evaluated the ferritinophagy level. We found that the expression of NCOA4 and heavy chain of ferritin (H-ferritin) were decreased to 25.4% and 35.8% in the liver of HFD mice (Fig. 5A and B) while showed increased in the PA treated HepG2 cells (Fig. 5E and F) compared to their control. In addition, the protein level of p62 (Fig. 5C and G) was increased and LIP (Fig. 5D and H) decreased significantly *in vivo and vitro*.

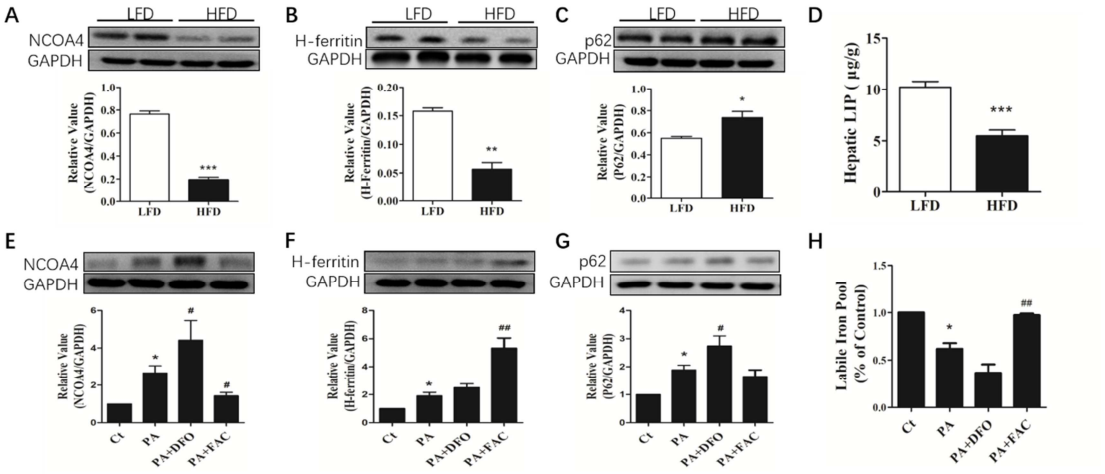


**Fig 5.** Ferritinophagy flux was suppressed *in vivo and in vitro*. The protein level of NCOA4, H-ferritin and p62 in both liver tissue (A, B, C) and HepG2 cells (E, F, G) were determined by Western blot (n=3). (D) LIP level in the mice liver was determined by flame atomic absorption spectrometry (n=8). (H) LIP level in HepG2 cells was determined by fluorescent dye Calcein-AM. The experiments were repeated 3 times. Values were presented as means ±SEM. * $p < 0.05$; ** $p<0.01$; ***: $p<0.001$ versus the LFD or Ct group. #: $p < 0.05$ versus the PA group.

Lysosome-associated membrane protein-2 (LAMP2) plays a critical role not only in lysosomal biogenesis but also in the maturation of autophagosomes and

phagosomes (Notomi et al., 2019). To further illustrate the effect of excess lipid intake on ferritinophagy, we did the co-staining assay *in vivo and in vitro*. As shown in Fig 6A, HFD decreased the co-localization of hepatic NCOA4, H-ferritin and LAMP2. Similar results were found in PA incubated HepG2 cells (Fig 6B). Furthermore, lysosomes activity as demonstrated by LysoTracker Red DND-99, and showed that PA decreased the lysosomes activity and FAC couldn't improve the lysosomes activity (Fig 6C).

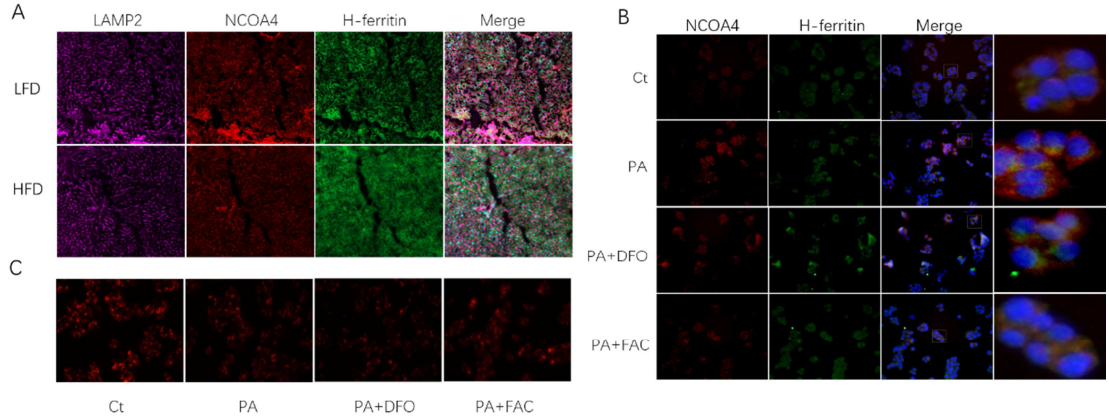


**Fig 6.** The co-staining of NCOA4 and H-ferritin. (A)Immunofluorescence with antibodies against NCOA4 (red), H-ferritin(green) and LAMP2 (pink) in the liver. (B)The co-staining of NCOA4 and H-ferritin was determined in HepG2 cells. (C) The lysosome activity was determined by LysoTracker Red DND-99 (LTR). The experiments were repeated 3 times (magnification 400X).

### 3.5 Impaired ferritinophagy flux-induced hepatic IR via ERS

Finally, we sought to determine whether the impaired ferritinophagy flux could induce hepatic IR. We enhanced or suppressed NCOA4 expression in HepG2 cells by either adenovirus-mediated gene transfer (Fig. 7A) or siRNA-mediated gene knockdown (Fig. 7C), respectively. NCOA4 overexpression improved glucose

uptake, while ERS induction by TG compromised this beneficial effect (Fig. 7B). Moreover, NCOA4 silencing inhibited glucose uptake even in the presence of FAC (Fig. 7D). Besides, ERS inhibition by 4-PBA or STF always improved glucose uptake whether NCOA4 is overexpressed or silenced. We also evaluated the effect of autophagy induction or inhibition on hepatic IR. MG-132, an inhibitor of the proteasome which can inhibit the proteasomal degradation of NCOA4 (De Domenico, Ward, & Kaplan, 2009). We found that MG-132 increased the expression of NCOA4 slightly and that wortmannin, an inhibitor for autophagosome formation reduced it obviously (Fig. 7F). Moreover, rapamycin, an inducer of autophagy, markedly decreased the p-IRE1α expression, while wortmannin does not affect the expression of p-IRE1α (Fig. 7G). Interestingly, autophagy induction by rapamycin improved glucose uptake while autophagy inhibition by bafilomycin A1 remarkedly enhanced the detrimental effect of PA (Fig. 7H).

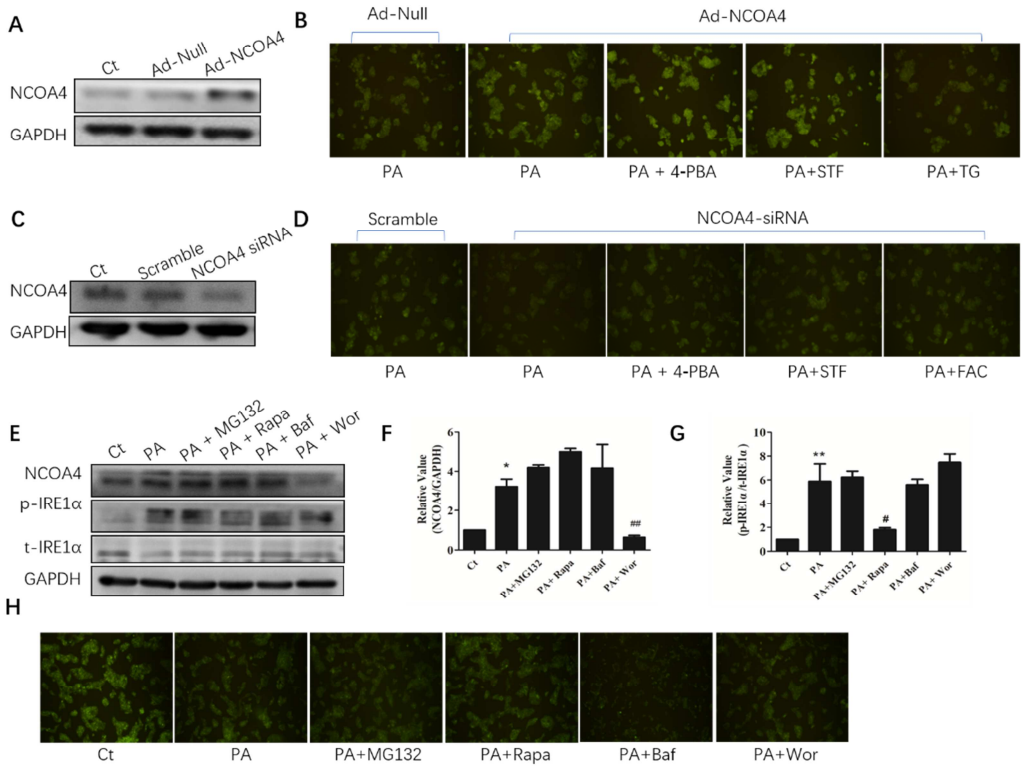


**Fig 7.** The impaired ferritinophagy flux induced hepatic IR via ERS. Western blots of the protein of NCOA4 expression in HepG2 cells after Ad-NCOA4 (A) or NCOA4 siRNA (C) transfection 48h. The glucose uptake of HepG2 cells (B, D). (E-G) The protein of NCOA4 and p-IRE1α. (H)The glucose uptake of HepG2 cells was observed. The experiments were repeated 3 times. Values were presented as means ± SEM. * $p < 0.05$; ** $p<0.01$ versus the LFD or Ct group. #: $p < 0.05$ versus the PA group.

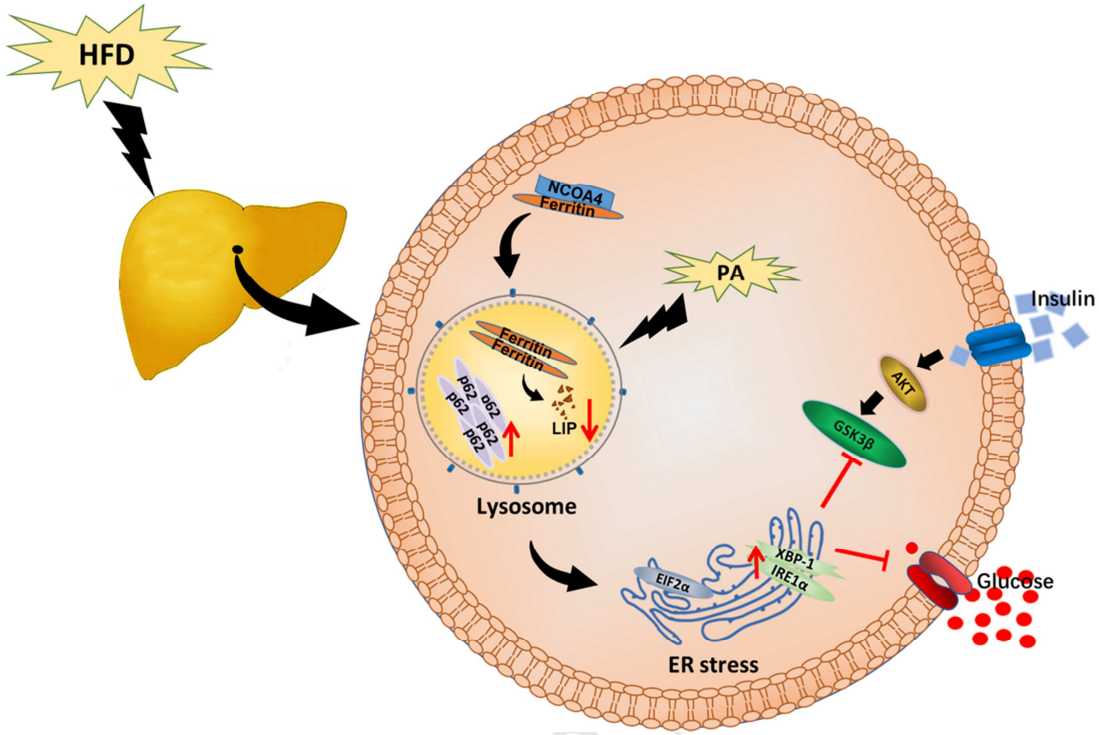


**Fig 8.** The proposed working mechanism involved in HFD-induced HIR. In the presence of HFD/PA, excess fat uptake by hepatocytes leads to the impaired function of the lysosome, which further suppressed ferritinophagy flux. Decreased LIP level results in the ERS. And that, the ERS is responsible for decreased glucose uptake and diminished expression of p-AKT and p-GSK3β, resulting in HIR. Collectively, impaired ferritinophagy flux induced by excess fat uptake leads to HIR via ERS.

## 4. Discussion

The major findings of our present study show that decreased iron level, ERS and impaired hepatic insulin signal occurred in the liver of HFD mice. Both iron deficiency and ERS could induce hepatic IR, and that iron supplementation rescued ERS and hepatic IR in PA-treated HepG2 cells. In addition, NCOA4 mediated ferritinophagy flux was also impaired and FAC restored the NCOA4 expression. We further provide evidence that NCOA4 overexpression improved ERS and hepatic IR

while its knockdown showed counterproductively. Thus, these together suggest that impaired ferritinophagy flux induced by HFD mediates hepatic insulin resistance via endoplasmic reticulum stress

Our findings have shown that mice administrated with HFD decreased H-ferritin expression (Fig. 3B) while HepG2 cells incubated with PA increased H-ferritin, compared with untreated controls. Thus, it seems paradoxical. It was reported that in both insulin model of Wistar rats and ob/ob obesity mice ferritin was observed decreased, and the higher iron demand and lower iron absorption may be involved this (Le Guenno, Chanseaume, Ruivard, Morio, & Mazur, 2007; MARK L. FAILLA, 1988). It was also reported that ectopic fat deposition leading to tissue iron redistribution may be the underlying mechanism of the lower iron level in the liver (Orr et al., 2014). And that decreased iron absorption by downregulating ferroportin (FPN) and divalent metal transporter 1 (DMT1) in the duodenum has been frequently reported in obesity or HFD mice(Chung, Kim, & Han, 2011; del Giudice et al., 2009; McClung & Karl, 2009; Sonnweber et al., 2012). It seems that different factors could lead to iron deficiency in the liver of HFD mice. Moreover, one study showed that H-ferritin increased while LIP declined in PA treated INS-1 beta cells (Jung et al., 2015).

It has been reported that iron content is higher in the liver of HFD mice and NAFLD patients and that the reduction of hepatic FPN expression induced by hepcidin may be the underlying mechanism (Aigner et al., 2008; Citelli et al., 2015). The iron level is tightly controlled, and the regulation of cellular and systemic iron

levels is highly sensitive and complex (Gozzelino & Arosio, 2016). These differences observed in iron content may be related to factors such as the intervention time and when the animal accepted the intervention, and even the breeding environment factors like the seasons. Even though the mechanisms for this discrepancy have not been fully understood yet, these conditions represent different manifestations of the same pathophysiological process (Aigner, Feldman, & Datz, 2014).

Ferritin degradation occurs in lysosomes, and this process is associated with autophagy (Huang et al., 2018). However, ferritinophagy as a newly discovered iron metabolism and regulation mechanism has not been reported in obesity or the HFD animal model. In current study, the disturbed NCOA4 and H-ferritin level, increased p62 expression and the reduced LIP level (Fig. 5) demonstrated that ferrinophagy flux was inhibited and that the available iron is deficient in the presence of HFD (PA). In line with these findings, iron supplementation rescued the NCOA4 express. Interestingly, the expression of NCOA4 and H-ferritin is consistent in vitro. As NCOA4 mediates ferritin degradation, this maybe indicates that the content of ferritin regulates the expression of NCOA4 or vice versa.

In the present study, autophagy induction by rapamycin increased the expression of NCOA4 and reduced ERS. In addition, wortmannin as an upstream inhibitor of autophagy reduced NCOA4 expression but showed no obvious effect on ERS and that bafilomycin A1 showed no obvious effect on NCOA4 and ERS. In addition, PA incubated HepG2 cells also exhibit impaired lysosome, as assessed by the fluorescent probe Red DND-99. This together suggests that impaired lysosomal function may be

the reason for suppressed ferritinophagy. However, iron supplementation shows no effect on the PH value of lysosome, indicating that FAC couldn't improve lysosomal function.

It was reported ferritin degradation occurs by 2 different routes: lysosome route and a cytosolic route in which iron is degraded by proteasome (De Domenico et al., 2009). In our present study, MG-132 increased the expression of NCOA4 slightly in PA incubated HepG2 cells, which might own to that the most of ferritin degraded by lysosomes route or the proteasome route also impaired in the presence of PA. On this point, further exploration is needed.

It was reported that iron deficiency could induce ERS which is a powerful mediator of insulin resistance (Seo et al., 2013; Yaribeygi, Farrokhi, Butler, & Sahebkar, 2019). DNA microarray analysis in the liver of rats found that genes of caspases 3 and 12, which could mediate endoplasmic reticulum (ER)-specific apoptosis, were upregulated in the iron-deficient dietary group(Ahmed & Oates, 2013). Furthermore, increased lipogenesis was shown to induce intracellular accumulation of diacylglycerol and ceramide which are pivotal for ERS and subsequently IR and hepatic steatosis (Petersen et al., 2017). In obesity, ERS could enhance the effects of insulin resistance, in which IRE1 lowers insulin responsiveness (W. Zhang, Hietakangas, Wee, Lim, Gunaratne, & Cohen, 2013). Herein, we found that PA increased the p-IRE1α expression, and FAC supplementation partially reversed its expression and glucose uptake in vitro. Thus, in addition to the ferritinophagy flux pathway, other mechanisms may also contribute to the ERS and hepatic IR.

## 5. Conclusion

In summary, these results revealed that suppressed ferritinophagy flux induced by excess lipid uptake is responsible for iron deficiency, which could contribute to the hepatic IR via ERS. What's more, iron supplementation has no obvious effect for the function of lysosomes but improved ERS and hepatic IR. Our findings contribute to a better understanding of the molecular mechanism of iron dysregulation in the liver of HFD mice and provide evidence and new insights for the prophylactic treatment of IR.

**Acknowledgments**

Gratitude is expressed to Dr. Yacoubou Abdoul Razak Mahaman from the Department of Pathology and Pathophysiology, Tongji Medical College for language revising.

**Author contributions**

Chunjie Jiang wrote the manuscript. Chunjie Jiang and Shanshan Zhang collected data and performed analysis. Dan Li, Li Chen, Ying Zhao and Guibin Mei fed mice, Chunjie Jiang and Jingjing Liu performed analysis. Ping Yao and Chao Gao designed the study. Ping Yao, Yuhan Tang and Chao Gao reviewed the manuscript.

**Financial support**

This work was supported by the National Natural Science Foundation of China (No. 81472979, 81973044, 81673164 and 81602858)

**Conflicts of interest**

The authors declare that there are no conflicts of interest.

## References

Ahmed, U., & Oates, P. S. (2013). Dietary fat level affects tissue iron levels but not the iron regulatory gene HAMP in rats. *Nutr Res, 33*(2), 126-135. https://doi.org/10.1016/j.nutres.2012.11.012.

Aigner, E., Feldman, A., & Datz, C. (2014). Obesity as an emerging risk factor for iron deficiency. *Nutrients, 6*(9), 3587-3600. https://doi.org/10.3390/nu6093587.

Aigner, E., Theurl, I., Theurl, M., Lederer, D., Haufe, H., Dietze, O., . . . Weiss, G. (2008). Pathways underlying iron accumulation in human nonalcoholic fatty liver disease. *Am J Clin Nutr, 87*(5), 1374-1383. https://doi.org/10.1093/ajcn/87.5.1374.

Arosio, P., Ingrassia, R., & Cavadini, P. (2009). Ferritins: a family of molecules for iron storage, antioxidation and more. *Biochim Biophys Acta, 1790*(7), 589-599. https://doi.org/10.1016/j.bbagen.2008.09.004.

Bellelli, R., Castellone, M. D., Guida, T., Limongello, R., Dathan, N. A., Merolla, F., . . . Carlomagno, F. (2014). NCOA4 transcriptional coactivator inhibits activation of DNA replication origins. *Molecular Cell, 55*(1), 123-137. https://doi.org/10.1016/j.molcel.2014.04.031.

Bellelli, R., Federico, G., Matte', A., Colecchia, D., Iolascon, A., Chiariello, M., . . . Carlomagno, F. (2016). NCOA4 Deficiency Impairs Systemic Iron Homeostasis. *Cell Reports, 14*(3), 411-421. http://dx.doi.org/10.1016/j.celrep.2015.12.065.

Cheng, H. L., Bryant, C., Cook, R., O'Connor, H., Rooney, K., & Steinbeck, K. (2012). The relationship between obesity and hypoferraemia in adults: a systematic review. *Obes Rev, 13*(2), 150-161. https://doi.org/10.1111/j.1467-789X.2011.00938.x.

Chung, J., Kim, M. S., & Han, S. N. (2011). Diet-induced obesity leads to decreased hepatic iron storage in mice. *Nutr Res, 31*(12), 915-921. https://doi.org/10.1016/j.nutres.2011.09.014.

Citelli, M., Fonte-Faria, T., Nascimento-Silva, V., Renovato-Martins, M., Silva, R., Luna, A. S., . . . Barja-Fidalgo, C. (2015). Obesity promotes alterations in iron recycling. *Nutrients, 7*(1), 335-348. https://doi.org/10.3390/nu7010335.

De Domenico, I., Ward, D. M., & Kaplan, J. (2009). Specific iron chelators determine the route of ferritin degradation. *Blood, 114*(20), 4546-4551. https://doi.org/10.1182/blood-2009-05-224188.

del Giudice, E. M., Santoro, N., Amato, A., Brienza, C., Calabro, P., Wiegerinck, E. T., . . . Perrone, L. (2009). Hepcidin in Obese Children as a Potential Mediator of the Association between Obesity and Iron Deficiency. *Journal of Clinical Endocrinology & Metabolism, 94*(12), 5102-5107. https://doi.org/10.1210/jc.2009-1361.

Gozzelino, R., & Arosio, P. (2016). Iron Homeostasis in Health and Disease. *International Journal of Molecular Sciences, 17*(1). https://doi.org/10.3390/ijms17010130.

Huang, T., Sun, Y., Li, Y., Wang, T., Fu, Y., Li, C., & Li, C. (2018). Growth Inhibition of a Novel Iron Chelator, DpdtC, against Hepatoma Carcinoma Cell Lines Partly Attributed to Ferritinophagy-Mediated Lysosomal ROS Generation. *Oxid Med Cell Longev, 2018*, 4928703. https://doi.org/10.1155/2018/4928703.

Jung, I. R., Choi, S. E., Jung, J. G., Lee, S. A., Han, S. J., Kim, H. J., . . . Kang, Y. (2015). Involvement of iron depletion in palmitate-induced lipotoxicity of beta cells. *Mol Cell Endocrinol, 407*, 74-84. https://doi.org/10.1016/j.mce.2015.03.007.

Kamei, A., Watanabe, Y., Ishijima, T., Uehara, M., Arai, S., Kato, H., . . . Abe, K. (2010). Dietary iron-deficient anemia induces a variety of metabolic changes and even apoptosis in rat liver: a DNA microarray study. *Physiol Genomics, 42*(2), 149-156. https://doi.org/10.1152/physiolgenomics.00150.2009.

Kim, J. L., Lee, D. H., Na, Y. J., Kim, B. R., Jeong, Y. A., Lee, S. I., . . . Min, B. W. (2016). Iron chelator-induced apoptosis via the ER stress pathway in gastric cancer cells. *Tumour Biol, 37*(7), 9709-9719. https://doi.org/10.1007/s13277-016-4878-4.

Kim, O. K., Jun, W., & Lee, J. (2015). Mechanism of ER Stress and Inflammation for Hepatic Insulin Resistance in Obesity. *Ann Nutr Metab, 67*(4), 218-227. https://doi.org/10.1159/000440905.

Konijn, A. M., Glickstein, H., Vaisman, B., Meyron-Holtz, E. G., Slotki, I. N., & Cabantchik, Z. I. (1999). The cellular labile iron pool and intracellular ferritin in K562 cells. *Blood, 94*(6), 2128-2134. https://www.ncbi.nlm.nih.gov/pubmed/10477743.

Kwon, B., Lee, H.-K., & Querfurth, H. W. (2014). Oleate prevents palmitate-induced mitochondrial dysfunction, insulin resistance and inflammatory signaling in neuronal cells. *Biochimica et Biophysica Acta (BBA) - Molecular Cell Research, 1843*(7), 1402-1413. https://doi.org/10.1016/j.bbamcr.2014.04.004.

Le Guenno, G., Chanseaume, E., Ruivard, M., Morio, B., & Mazur, A. (2007). Study of iron metabolism disturbances in an animal model of insulin resistance. *Diabetes Res Clin Pract, 77*(3), 363-370. https://doi.org/10.1016/j.diabres.2007.02.004.

Lee, J. M. (2017). Nuclear Receptors Resolve Endoplasmic Reticulum Stress to Improve Hepatic Insulin Resistance. *Diabetes Metab J, 41*(1), 10-19.

https://doi.org/10.4093/dmj.2017.41.1.10.

Liu, P., Lin, H., Xu, Y., Zhou, F., Wang, J., Liu, J., . . . Yao, P. (2018). Frataxin-Mediated PINK1-Parkin-Dependent Mitophagy in Hepatic Steatosis: The Protective Effects of Quercetin. *Mol Nutr Food Res, 62*(16), e1800164. https://doi.org/10.1002/mnfr.201800164.

Magnusson, I., Rothman, D. L., Katz, L. D., Shulman, R. G., & Shulman, G. I. (1992). Increased rate of gluconeogenesis in type II diabetes mellitus. A 13C nuclear magnetic resonance study. *Journal of Clinical Investigation, 90*(4), 1323-1327. https://doi.org/10.1172/JCI115997.

Mancias, J. D., Wang, X., Gygi, S. P., Harper, J. W., & Kimmelman, A. C. (2014). Quantitative proteomics identifies NCOA4 as the cargo receptor mediating ferritinophagy. *Nature, 509*(7498), 105-109. https://doi.org/10.1038/nature13148.

Manios, Y., Moschonis, G., Chrousos, G. P., Lionis, C., Mougios, V., Kantilafti, M., . . . Katsarou, C. (2013). The double burden of obesity and iron deficiency on children and adolescents in Greece: the Healthy Growth Study. *J Hum Nutr Diet, 26*(5), 470-478. https://doi.org/10.1111/jhn.12025.

MARK L. FAILLA, M. L. K., MINGL CHEN. (1988). Iron Metabolism in Genetically Obese (obob) Mice.pdf. *American Institute of Nutrition, 118*(1), 46–51. https://doi.org/https://doi.org/10.1093/jn/118.1.46.

McClung, J. P., & Karl, J. P. (2009). Iron deficiency and obesity: the contribution of inflammation and diminished iron absorption. *Nutr Rev, 67*(2), 100-104. https://doi.org/10.1111/j.1753-4887.2008.00145.x.

Notomi, S., Ishihara, K., Efstathiou, N. E., Lee, J. J., Hisatomi, T., Tachibana, T., . . . Vavvas, D. G. (2019). Genetic LAMP2 deficiency accelerates the age-associated formation of basal laminar deposits in the retina. *Proc Natl Acad Sci U S A*. https://doi.org/10.1073/pnas.1906643116.

Orr, J. S., Kennedy, A., Anderson-Baucum, E. K., Webb, C. D., Fordahl, S. C., Erikson, K. M., . . . Hasty, A. H. (2014). Obesity alters adipose tissue macrophage iron content and tissue iron distribution. *Diabetes, 63*(2), 421-432. https://doi.org/10.2337/db13-0213.

Petersen, M. C., & Shulman, G. I. (2017). Roles of Diacylglycerols and Ceramides in Hepatic Insulin Resistance. *Trends Pharmacol Sci, 38*(7), 649-665. https://doi.org/10.1016/j.tips.2017.04.004.

Quiles Del Rey, M., & Mancias, J. D. (2019). NCOA4-Mediated Ferritinophagy: A Potential Link to Neurodegeneration. *Front Neurosci, 13*(238), 238. https://doi.org/10.3389/fnins.2019.00238.

Samuel, V. T., & Shulman, G. I. (2016). The pathogenesis of insulin resistance: integrating signaling pathways and substrate flux. *The Journal of Clinical Investigation, 126*(1), 12-22. https://doi.org/10.1172/JCI77812.

Seo, Y. A., Li, Y., & Wessling-Resnick, M. (2013). Iron depletion increases manganese uptake and potentiates apoptosis through ER stress. *Neurotoxicology, 38*, 67-73. https://doi.org/10.1016/j.neuro.2013.06.002.

Simcox, J. A., & McClain, D. A. (2013). Iron and diabetes risk. *Cell Metab, 17*(3), 329-341. https://doi.org/10.1016/j.cmet.2013.02.007.

Sonnweber, T., Ress, C., Nairz, M., Theurl, I., Schroll, A., Murphy, A. T., . . . Weiss, G. (2012). High-fat diet causes iron deficiency via hepcidin-independent reduction of duodenal iron absorption. *The Journal of Nutritional Biochemistry, 23*(12), 1600-1608. https://doi.org/https://doi.org/10.1016/j.jnutbio.2011.10.013.

Sturm, B., Goldenberg, H., & Scheiber-Mojdehkar, B. (2003). Transient increase of the labile iron pool in HepG2 cells by intravenous iron preparations. *Eur J Biochem, 270*(18), 3731-3738. https://doi.org/10.1046/j.1432-1033.2003.03759.x.

Tang, Y., Li, Y., Yu, H., Gao, C., Liu, L., Xing, M., . . . Yao, P. (2014). Quercetin attenuates chronic ethanol hepatotoxicity: implication of "free" iron uptake and release. *Food Chem Toxicol, 67*, 131-138. https://doi.org/10.1016/j.fct.2014.02.022.

Yaribeygi, H., Farrokhi, F. R., Butler, A. E., & Sahebkar, A. (2019). Insulin resistance: Review of the underlying molecular mechanisms. *J Cell Physiol, 234*(6), 8152-8161. https://doi.org/10.1002/jcp.27603.

Yu, X., Deng, Q., Tang, Y., Xiao, L., Liu, L., Yao, P., . . . Dong, X. (2018). Flaxseed Oil Attenuates Hepatic Steatosis and Insulin Resistance in Mice by Rescuing the Adaption to ER Stress. *J Agric Food Chem, 66*(41), 10729-10740. https://doi.org/10.1021/acs.jafc.8b03906.

Zhang, Q., Yuan, H., Zhang, C., Guan, Y., Yuqing Wu, Fan Ling, . . . Li, Y. (2018). Epigallocatechin gallate improves insulin resistance in HepG2 cells through alleviating inflammation and lipotoxicity. *Diabetes Research and Clinical Practice, 142*, 363-373. https://doi.org/10.1016/j.diabres.2018.06.017.

Zhang, W., Hietakangas, V., Wee, S., Lim, S. C., Gunaratne, J., & Cohen, S. M. (2013). ER

stress potentiates insulin resistance through PERK-mediated FOXO phosphorylation. *Genes Dev, 27*(4), 441-449. https://doi.org/10.1101/gad.201731.112.

Zhao, R., Fuentes-Mattei, E., Velazquez-Torres, G., Su, C. H., Chen, J., Lee, M. H., & Yeung, S. C. (2011). Exenatide improves glucocorticoid-induced glucose intolerance in mice. *Diabetes Metab Syndr Obes, 4*, 61-65. https://doi.org/10.2147/DMSO.S15510.

Zhou, Y., Wu, W., Xu, Z., Liu, Y., Chang, H., Yu, P., . . . Chang, Y. (2019). Iron regulatory protein 2 deficiency may correlate with insulin resistance. *Biochem Biophys Res Commun, 510*(2), 191-197. https://doi.org/10.1016/j.bbrc.2019.01.022.

Zhu, X., Xiong, T., Liu, P., Guo, X., Xiao, L., Zhou, F., . . . Yao, P. (2018). Quercetin ameliorates HFD-induced NAFLD by promoting hepatic VLDL assembly and lipophagy via the IRE1a/XBP1s pathway. *Food Chem Toxicol, 114*, 52-60. https://doi.org/10.1016/j.fct.2018.02.019.

Zhu, X., Yao, P., Liu, J., Guo, X., Jiang, C., & Tang, Y. (2020). Baicalein attenuates impairment of hepatic lysosomal acidification induced by high fat diet via maintaining V-ATPase assembly. *Food Chem Toxicol, 136*, 110990. https://doi.org/10.1016/j.fct.2019.110990.

1. HFD suppressed ferritinophagy flux.
2. Impaired ferritinophagy flux aggravates hepatic IR via ERS
3. Impaired lysosomal function involves in the suppressed ferritinophagy flux

**Declaration of interests**

☒ The authors declare that they have no known competing financial interests or personal relationships that could have appeared to influence the work reported in this paper.

☐The authors declare the following financial interests/personal relationships which may be considered as potential competing interests: